Photosynth Res (2008) 96:51–60
DOI 10.1007/s11120-007-9283-9

REGULAR PAPER

Purification of His_6-tagged Photosystem I from *Chlamydomonas reinhardtii*

Galina Gulis · Kuppala V. Narasimhulu · Lisa N. Fox · Kevin E. Redding

Received: 24 September 2007 / Accepted: 10 December 2007 / Published online: 4 January 2008

Abstract We have developed a rapid method for isolation of the Photosystem I (PS1) complex from *Chlamydomonas reinhardtii* using epitope tagging. Six histidine residues were genetically added to the N-terminus of the PsaA core subunit of PS1. The His_6-tagged PS1 could be purified with a yield of 80–90% from detergent-solubilized thylakoid membranes within 3 h in a single step using a Ni-nitrilotriacetic acid (Ni-NTA) column. Immunoblots and low-temperature fluorescence analysis indicated that the His_6-tagged PS1 preparation was highly pure and extremely low in uncoupled pigments. Moreover, the introduced tag appeared to have no adverse effect upon PS1 structure/function, as judged by photochemical assays and EPR spectroscopy of isolated particles, as well as photosynthetic growth tests of the tagged strain.

Keywords His-tag · Epitope tagging · Membrane protein · Reaction center · Photosystem 1 · *Chlamydomonas reinhardtii*

Electronic supplementary material The online version of this article (doi:10.1007/s11120-007-9283-9) contains supplementary material, which is available to authorized users.

G. Gulis · K. V. Narasimhulu · L. N. Fox · K. E. Redding (✉)
Departments of Chemistry and Biological Sciences, University of Alabama, 206 Shelby Hall, 250 Hackberry Lane, Tuscaloosa, AL 35487-0336, USA
e-mail: kevin.redding@ua.edu

Present Address:
K. E. Redding
Institute de Biologie Physico-Chimique, 13 rue Pierre et Marie Curie, Paris 75005, France

Introduction

Photosystem I (PS1) is one of the major membrane protein complexes of the chloroplast involved in photosynthesis, along with Photosystem II (PS2), light harvesting complexes (LHC), cytochrome b_6f (cyt b_6f) and ATP synthase (ATPase). The core subunits of PS1, PsaA, and PsaB, are incorporated into the thylakoid membrane of the chloroplast and serve as a scaffold for the pigments and cofactors required for absorption and use of photons to drive electron transfer from plastocyanin to ferredoxin. The crystal structure of cyanobacterial PS1 at 2.5-Å resolution revealed that 12 protein subunits (PsaA to PsaF, PsaI to PsaM and PsaX), 96 chlorophyll *a* molecules, 22 carotenoids, 2 phylloquinones, and 3 Fe_4S_4 clusters are present (Jordan et al. 2001). The structure of eukaryotic PS1 is remarkably similar at the core, although it lacks the cyanobacterial subunits PsaM and PsaX and has subunits PsaG, PsaH, and PsaN (Amunts et al. 2007; Ben-Shem et al. 2003). It also possesses a belt of LHCI subunits on one side of the complex, which increases the light-harvesting capacity of PS1. The six N-terminal α-helices of PsaA and PsaB bind a large number of chlorophyll *a* molecules and carotenoids, whose role is to harvest photons and transfer excitation energy to the reaction center. The five C-terminal α-helices form two semicircles cradling the initial electron transfer cofactors. In order these are: P_{700}, a heterodimer of Chl *a* and Chl *a*′; a pair of chlorophyll *a* molecules (ec2 and ec3); a phylloquinone (PhQ); and F_X, an Fe_4S_4 cluster (Jordan et al. 2001). The terminal electron acceptors, the Fe_4S_4 clusters F_A and F_B, are bound by the extrinsic subunit PsaC on the stromal side (Golbeck and Bryant 1991).

Unlike the situation in other organisms, the *psaA* gene is split into three separate exons in the *C. reinhardtii*

chloroplast genome, which are scattered around the circular chloroplast genome. Exon 1 (86 bp) is separated by ~50 kb from exon 2 (198 bp), which is positioned ~90 kb from exon 3 (1984 bp) (Kück et al. 1987) (see Fig. 1). The three separate exon transcripts are linked together to form the mature *psaA* mRNA by a post-transcriptional *trans*-splicing process resembling that in group II introns (Goldschmidt-Clermont et al. 1990; Perron et al. 2004).

Isolation and purification of membrane protein complexes can be an inefficient and time-consuming process. Typically, PS1 has been purified by use of sucrose-density gradients after detergent solubilization, usually β-dodecylmaltoside (Hippler et al. 1997; Takahashi et al. 1991). Good success has also been had with purification by column chromatography, including the use of weak anion exchange (Ramesh and Webber 2004) and molecular sieve (Krabben et al. 2000) matrices. In order to develop a new way to purify PS1 rapidly and with a high yield, we employed an epitope-tagging strategy. We chose to use the His_6-tag, as it has previously been used to good result with the photosynthetic reaction center of purple bacteria (Goldsmith et al. 1996) and PS2 of *C. reinhardtii* (Sugiura et al. 1998).

We reasoned that the N-terminus of PsaA subunit would be an excellent target for attachment of the tag for several reasons. First, the N-terminus of either PsaA or PsaB would be on the periphery of the protein and unlikely to interfere with core electron transfer processes (Fig. 1a). Second, the N-terminus of PsaA seems to be unstructured, since the first 12 amino acid residues are not resolved in the crystal structure of *T. elongatus* (Jordan et al. 2001). Thus, the N-terminus of PsaA does not appear to be a critical portion of the PS1 structure, which is consistent with the fact that it is not well conserved between species (see Fig. 1b). Third, the introduction of the His_6-tag to the first exon of *psaA* would ease subsequent creation of tagged PS1 with directed mutations elsewhere, as detailed further in the Discussion.

Materials and methods

Materials

Restriction endonucleases and DNA polymerases were purchased from New England Biolabs. Gold carriers were

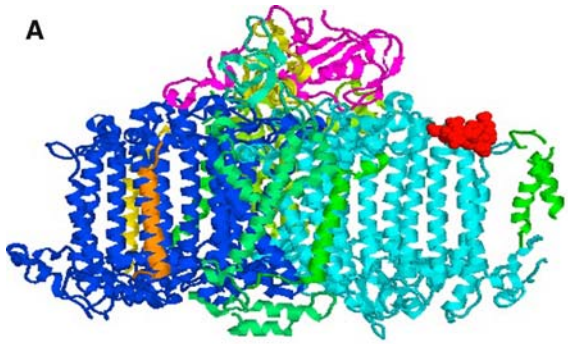

B

```
PSAA_CHLRE      MTISTPER--E---AKKVKIAVDRNPVETSFEKWAKPGHFSRTLSKGPNTTTWIWNLHA
PSAA_SYNEN      MTISPPER--E---PK-VRVVVDNDPVPTSFEKWAKPGHFDRTLARGPQTTTWIWNLHA
PSAA_ARATH      MIIRSPEP--------EVKILVDRDPIKTSFEEWAKPGHFSRTIAKGPDTTTWIWNLHA
PSAA_PEA        MIIRSPEPKVQILADPEVKILVDRDPIKTSFEQWAKPGHFSRTIAKGPDTTTWIWNLHA
PSAA_ORYSA      MMIRSPEP--------EVKIVVDRDPVKTSFEEWARPGHFSRTLAKGPDTTTWIWNLHA
PSAA_PINTH      MTIRSPEP--E---VKKVKVVVDRDTVKTSFEKWAKPGHFSRTLAKGPDTTTWIWNLHA
PSAA_MARPO      MTIRSPEP--------EVKIVVEKDPVKTSFEKWAKPGHFSRTLAKGPSTTTWIWNLHA
PSAA_EUGGR      MTITPPEQ--Q---VKRVRVAFVSNPVETSFEKWSRPGHFSRLLSKGPNTTTWIWNLHA
PSAA_ODOSI      MAISSTER--R---AKNVQIFVEKDAVETSFAKWAQPGHFSRTLAKGPKTTTWIWNLHA
PSAA_PORPU      MAISSKEQ--E---TKKVKISVDKNPVDTSFEKWAQPGHFSRTLAKGPKTTTWIWNLHA
PSAA_CYAPA      MRISPPER--E---AKKVKIVIDKDPVSTSFDKWAVPGHFSRTLAKGPKTTTWIWNLHA
PSAA_ANASQ      MTISPPER--E---EKKARVIVDKDPVPTSFEKWAQPGHFDRTLARGPKTTTWIWNLHA
PSAA_MASLA      MTISPPER--E---EKKARVIVDNDPVPTSFELWAKPGHFDRTLARGPKTTTWIWNLHA
PSAA_SYNP2      M----------A--VK--VDKDPVPTSFEKWGKPGHFDRTLARGPKTTTWIWNLH A
```

Fig. 1 Placement of His_6-tag. (Panel **a**) Model of PS1 from *Thermosynechococcus elongatus*. The core subunits PsaA (cyan), PsaB (blue) and the extrinsic subunits PsaC (yellow), PsaD (magenta), PsaE (blue-green) are shown as ribbon cartoons. Residues #13–20 of PsaA are shown as a space-filling model in red. (Panel **b**) Alignments of PsaA N-termini from selected species. The sequences from *C. reinhardtii* (CHLRE) and *T. elongatus* (SYNEN) are shown on top, with several other species for comparison (ARATH, *Arabidopsis thaliana*; ORYSA, *Oryza sativa*; PINTH, *Pinus thunbergii*; MARPO, *Marchantia polymorpha*; EUGGR, *Euglena gracilis*; ODOSI, *Odontella sinensis*; PORPU, *Porphyra purpurea*; CYAPA, *Cyanophora paradoxa*; ANASQ, *Anabaena variabilis*; MASLA, *Mastigocladus laminosus*; SYNP2, *Synechococcus* sp. PCC 7002). The residues encoded by exon 1 in *C. reinhardtii* are indicated in red

obtained from Seashell Technology LLC. Ni-NTA agarose was obtained from Invitrogen. Antibodies against PsbA, Lhca1, Lhcb1, cyt *f*, and AtpB were obtained from Agri-Sera. The detergent β-D-dodecylmaltoside (β-DM) was obtained from Dojindo Laboratories. All chemicals used were of reagent grade.

Creation of His_6-tagged psaA-exon1

Exon 1 of *psaA* was cloned by ligating a ~2.7-kbp *Spe*I–*Eco*RI fragment from plasmid p-57 (Rochaix 1978) into pBluescript (Stratagene) cut with the same enzymes to generate plasmid pNF1. The His_6-tag was inserted by performing a PCR using pNF1 as template and two primers: ex1 (GTACCACTTTGGGAGAGGGTATT) and ex1-H6 (ACTGTGGTGGTGGTGGTGGTGAATTGTCATGG ATTT). The resulting PCR product corresponds to a region upstream of the open reading frame, along with the 4 first codons of PsaA, and with 6 His codons inserted between the third and fourth codon (See Fig. 2). The PCR product was digested with *Nhe*I, which cuts 408 bp upstream of the start codon. Fortuitously, the fourth and fifth codons compose a *Sca*I site (AGTACT), so that the PCR product would correspond to the product of *Sca*I cleavage at the 3′ end. Unfortunately, there is a second *Sca*I site in pNF1, located in the *bla* gene. Accordingly, pNF1 was cut with *Nhe*I and *Sca*I, and the ~3.3-kb *Sca*I–*Sca*I fragment and the ~2.8-kb *Sca*I–*Nhe*I fragment were recovered. These were ligated to the 438-bp *Sca*I–*Nhe*I insert created by PCR, and ampicillin-resistant colonies were selected after transformation into DH5α. Putative positive clones were identified by a slightly longer PCR product: 231 vs. 213 bp using primers ex1-H6 (ACTGTGGTGGTGGTGGTGGTG AATTGTCATGGATTT) and ex1-3′UTR (CGGCCAA-CAGTGCTTAAAAC). Plasmid DNA was isolated from them and verified by restriction digests and sequencing.

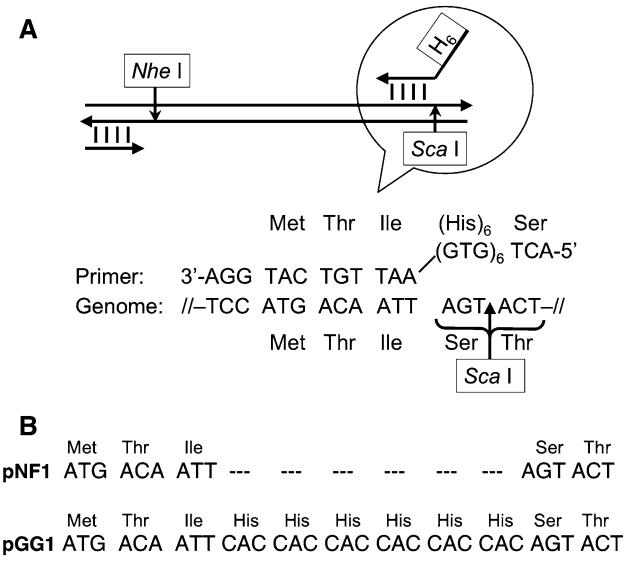

Fig. 2 Introducing the His_6-tag by PCR. (Panel **A**) Arrows indicate directions of primers (5′→3′). Primer and genomic sequences at site of His_6-tag are shown below. (Panel **B**) Sequence of WT and His_6-tagged exon1

A confirmed plasmid (pGG1) was mixed with pORF472::*aadA* (Fischer et al. 1996) at a ratio of 5:1, adsorbed onto ~1-µm gold carriers (SO4e gold, Seashell Technology) according to the manufacturer's instructions, and shot into wild-type (WT) *C. reinhardtii* strain JVD-1B (obtained from J. van Dillewijn and J-D. Rochaix, U. Geneva) using a home-built helium gun. Transformants were selected on TAP plates supplemented with 100 µg/ml spectinomycin and transferred to plates containing 50 µg/ml streptomycin to verify transformation with *aadA*. DNA was prepared from transformants and analyzed by PCR using oligonucleotides ex1-5'UTR-s (AAATAATTGTT ATTATAAGGAGAAATCC) and ex1-as (CGGCCAACA GTGCTTAAAAC) to detect co-transformants harboring the His_6-tagged exon 1 of *psaA*.

Algae strain growth

Algae were grown photo-heterotrophically at 25°C in well-aerated liquid TAP (Tris–acetate–phosphate) medium (Harris 1989). For growth tests, all strains were grown in TAP media for 3 days in dim light (~1 µEinstein m^{-2} s^{-1}). Cells were collected by centrifugation (10 min at 2300 × *g*) and diluted to 1–2 × 10^6 cells/ml before deposition on agar plates containing either TAP medium or a medium in which the acetate was replaced by 25 mM sodium bicarbonate. Plates were incubated at 25°C in the dark, medium light (50 µEinstein m^{-2} s^{-1}) and high light (200 µEinstein m^{-2} s^{-1}). Pictures were taken with a FluorS MultiImager (Bio-Rad) using a cooled CCD camera and red filter.

Preparation of thylakoid membranes and PS1 by sucrose gradients

Cells were harvested at a density of 4–5 × 10^6 cells ml^{-1} and thylakoid membranes were prepared as described (Fischer et al. 1997). Chlorophyll concentrations were measured spectrophotometrically after extraction with 80% acetone (Porra et al. 1989). Protein concentration was measured by the bicinchoninic acid assay (Smith et al. 1985).

PS1 particles from the WT strain were isolated by following a modified protocol from Fisher et al. (1997). Thylakoid membranes from the JVD1-1B strain were

diluted to 0.8 (mg Chl) ml^{-1} with water and solubilized by addition of 1/10 volume of 10% β-DM in the dark for 20 min on ice. Solubilized membranes were spun at 24,000*g* for 15 min at 4°C in a type 70Ti rotor. The supernatant (2 ml) was loaded onto a sucrose gradient formed by thawing a tube that had been frozen after layering 2 ml of 2 M sucrose, 10 ml of 0.9 M sucrose, and 10 ml of 0.5 M sucrose (all containing 5 mM Tricine–KOH (pH 8.0) and 0.05% β-DM). After spinning for 12 h at 150,000*g* in a type 70Ti rotor at 4°C, three green bands were collected: top fraction (LHC2), middle fraction (PS2/PS1), and bottom fraction (PS1). After dilution with at least 2 volumes of 5 mM Tricine–NaOH (pH 8.0), particles were collected by centrifugation (3 h at 250,000*g*, 4°C in a SW-55 rotor). Particles were frozen in liquid N_2 and stored at −70°C.

Purification of His_6-tagged PS1 (H_6-PS1) complex

Thylakoid membranes from JVD1-1B[pGG1-46] were harvested by centrifugation, resuspended at 0.8 mg Chl ml^{-1} in solubilization buffer (25 mM HEPES–KOH (pH 7.5), 100 mM NaCl, 5 mM $MgSO_4$, 10% glycerol) and solubilized by addition of 1/10 volume of 10% β-DM followed by gentle mixing for 30 min at 4°C. After centrifugation at 13,000*g* for 15 min at 4°C to remove unsolubilized material, 8 ml (1.6 mg of Chl) of the supernatant was loaded onto a Ni-NTA (Invitrogen) column (1.5 cm diameter × 12 cm height), which had been pre-equilibrated with column buffer (solubilization buffer + 0.03% β-DM). The column was washed with 130 ml column buffer containing 2 mM imidazole. The H_6-PS1 was eluted with column buffer containing 200 mM imidazole and 40 mM MES-NaOH (pH 6.0) instead of HEPES–KOH (pH 8.0), while collecting 5-ml fractions. Fractions were dialyzed 3 times against 2 l of solubilization buffer and concentrated by centrifugation (3 h at 250,000*g* in SW-55 rotor). All work was performed at 4°C.

Immunoblots

Thylakoid membranes from the His_6-tagged and WT strains, as well as PS1 particles prepared from them, were dissolved in Laemmli buffer and loaded onto NuPAGE 4–12% Bis–Tris gels (Invitrogen) at 2-μg Chl per lane. The resolved proteins were transferred onto Millipore Immobilon-P PVDF membranes and immunoblotting was performed using standard protocols with antisera against subunits of PS1 (PsaA (1:2000), PsaD (1:5000), PsaE (1:2000), PsaF (1:2000); (Boudreaux et al. 2001)) and other proteins using dilutions as specified by the manufacturer.

Flash spectroscopy

Particles were diluted to ~30 μM Chl in a buffer containing 120-mM Tricine (pH 8.0), 10 mM $MgCl_2$, 0.03% β-DM, 10 mM sodium ascorbate, and 200 μM dichlorophenolindophenol. They were placed in matched cuvets of a home-built Joliot-type double-beam spectrometer, essentially as described in (Joliot et al. 1980). Saturating actinic flashes (to only one of the cuvets) were provided by a Xe lamp filtered by a combination of 3-mm BG25 and 1-mm BG39 filters (Schott). Detection flashes were passed through a monochromator and split before the samples, and a Schott RG645 filter was placed in front of each detector to eliminate actinic light.

Low-temperature fluorescence

Thylakoid membranes and purified PS1 particles were processed for low-temperature fluorescence, as described (Henderson et al. 2003). B-phycoerythrin (5 μg/ml) was included as an internal standard to allow normalization of the emission spectra using excitation at 467 nm.

Electron Paramagnetic Resonance (EPR) spectroscopy

PS1 particles were frozen under illumination to generate the P_{700}^{+} $(F_A/F_B)^{-}$ state. The echo-detected field-swept (EDFS) EPR spectra were collected on an ELEXSYS-E680 EPR spectrometer equipped with an electrically controlled Oxford liquid He transfer line attached to a rectangular type cryostat to maintain the sample at 9 K. The EDFS-EPR spectra were measured with a two-pulse echo sequence ($\pi/2 - \tau - \pi - \tau -$ echo). Microwave pulse lengths of 16 and 32 ns were used with $\tau = 180$ ns, and with a repetition rate of 0.5 kHz.

Photochemical activity assay

A Clark-type oxygen electrode was used to measure O_2 uptake rates by PS1 particles using 5 mM sodium ascorbate, as electron donor (with 0.2 mM dichlorophenolindophenol as mediator) and 0.8 mM methyl viologen as mediator to O_2 as described (Takahashi et al. 1991). Red LED arrays ($\lambda_{avg} = 650 \pm 50$ nm) were used as a source of actinic light with different light fluxes. Double-reciprocal plots were used to estimate the maximal velocity.

Results

Cloning strategy

A portion of the *C. reinhardtii* chloroplast genome containing *psaA* exon 1 was first subcloned into a high-copy plasmid (see Materials and Methods). This was used as a template for the PCR to create the His_6-tagged N-terminus (Fig. 2a). The resulting PCR product contained DNA upstream of exon 1 along with the first four codons and 6 His codons inserted between the third and fourth codon. Since the fourth and fifth codons of exon 1 comprise a *Sca*I site, the PCR product at this end would correspond to the product of digestion by *Sca*I, which is a blunt-cutter. The pNF1 vector was digested with *Sca*I and an upstream site (*Nhe*I), and the insert, which was also digested with *Nhe*I, was ligated to it to make the plasmid pGG1. The sequence of exon 1 and the upstream region were confirmed by sequencing to correspond to the expected sequence (Fig. 2b).

Creation and characterization of His_6-tagged strain

A mixture of the pGG1 plasmid and the pORF472::*aadA* plasmid was introduced bio-ballistically into a *C. reinhardtii* WT strain. This allows for both the initial selection of the *aadA* marker and its subsequent loss (Fischer et al. 1996). Transformants were selected for resistance to spectinomycin and verified by streptomycin-resistance, since the *aadA* gene product confers resistance to both aminoglycoside antibiotics (Goldschmidt-Clermont 1991). They were then screened for presence of the His_6-tag by PCR, which produced products of 213 bp (WT) or 231 bp (His_6-tag), which could be easily distinguished (data not shown). Positive co-transformants were monitored by PCR during several rounds of sub-cloning after selective pressure was dropped to ensure that the His_6-tag was homoplasmic (i.e., all WT copies of the *psaA* exon 1 had been replaced).

We first tested the possibility that the His_6-tag would cause a gross defect in PS1 structure and/or function. This was easy to do by simple growth tests, given the absolute dependence of this organism upon PS1 function during photosynthetic growth (Redding et al. 1999). Cultures of various strains were spotted on agar plates containing acetate or bicarbonate as carbon sources and grown under different light conditions. *C. reinhardtii* can grow heterotrophically on acetate in the dark, but photosynthesis is required to use bicarbonate. Moreover, low amounts of PS1 activity render algal cells photosensitive even under heterotrophic conditions (Redding et al. 1998, 1999). The His_6-tagged strain grew as well as the WT strain under all tested conditions (Fig. 3). As negative controls, we used

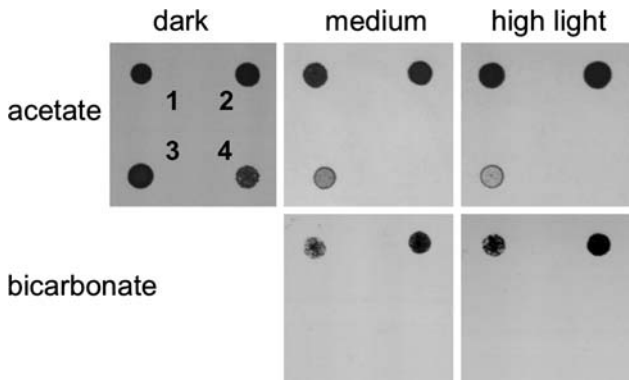

Fig. 3 Growth tests. Different strains were grown in liquid TAP medium under low light, spotted onto agar plates containing either acetate or bicarbonate as a carbon source, and then incubated at 25°C under low light (<0.1 μEinstein m^{-2} s^{-1}), medium light (50 μEinstein m^{-2} s^{-1}), or high light (200 μEinstein m^{-2} s^{-1}). Strains were: (1) WT, (2) His_6-tagged strain, (3) *psaA-H408Q* (containing PS1 at ~20% WT level; Redding et al. 1998), and (4) *psaA-3*Δ

strains with a mutant PS1 that is accumulated at ~20% the WT level (Redding et al. 1998) or lacking PS1 altogether (*psaA-3*Δ), demonstrating how obvious a gross defect in PS1 would manifest itself by this assay. These results were consistent with the fact that the tagged-PS1 strain appears to accumulate PS1 at normal levels (data not shown).

Purification of His_6-tagged PS1 (H_6-PS1)

Thylakoid membranes from the His_6-tagged strain were solubilized with β-DM and loaded on a Ni-NTA column. Most of the chlorophyll was washed from the column using 2 mM imidazole at pH 8, as expected, but a fraction remained bound until elution was carried out with 200 mM imidazole (pH 6). This buffer completely removed the bound chlorophyll in about 10 ml (2 fractions), and immunoblots indicated the presence of PS1 subunits in these fractions (Fig. 4a). The eluates contained more than 90% of the input PS1, as measured by immunoblots against the PsaA subunit. Note that WT PS1 without the His_6-tag did not bind to the column (Fig. 4b). After dialysis, the three most concentrated fractions (3–5) were pooled together and PS1 was concentrated by centrifugation. We obtained in total 1.2 mg of protein and 0.3 mg of Chl (*a*/*b* ratio = 7.5) from the input solubilized membranes, which had contained 24 mg of protein and 7.6 mg of Chl (*a*/*b* ratio = 2.2).

Purity of the H_6-PS1 preparation

H_6-PS1 particles and conventionally purified WT particles, along with the thylakoid membranes from which they were

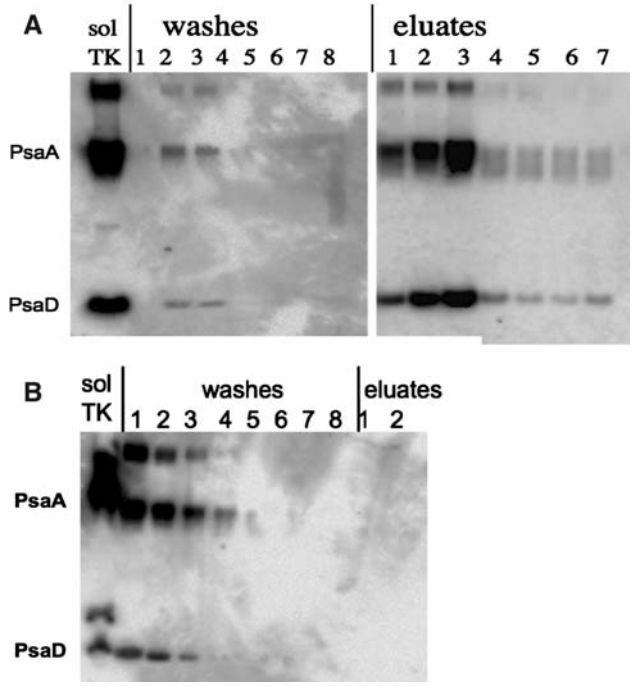

Fig. 4 Purification of His_6-tagged PS1 by Ni-NTA affinity chromatography. (Panel **A**) Purification of H_6-PS1. Immunoblot analysis of fractions that were washed from Ni-NTA column with 2 mM imidazole-containing buffer at pH 7.5 (left) and fractions that were eluted with 200 mM imidazole-containing buffer at pH 6.0 (right), compared to the input detergent-solubilized thylakoid membranes from the His_6-tagged strain. All fractions were loaded on 4–12% Bis–Tris Nu-PAGE by equal volume. (Panel **B**) Passage of unmodified PS1 through Ni-NTA column. Immunoblot analysis of fractions collected after washing and elution of detergent-solubilized thylakoid membranes of WT strain from Ni-NTA resin, using the same conditions as above

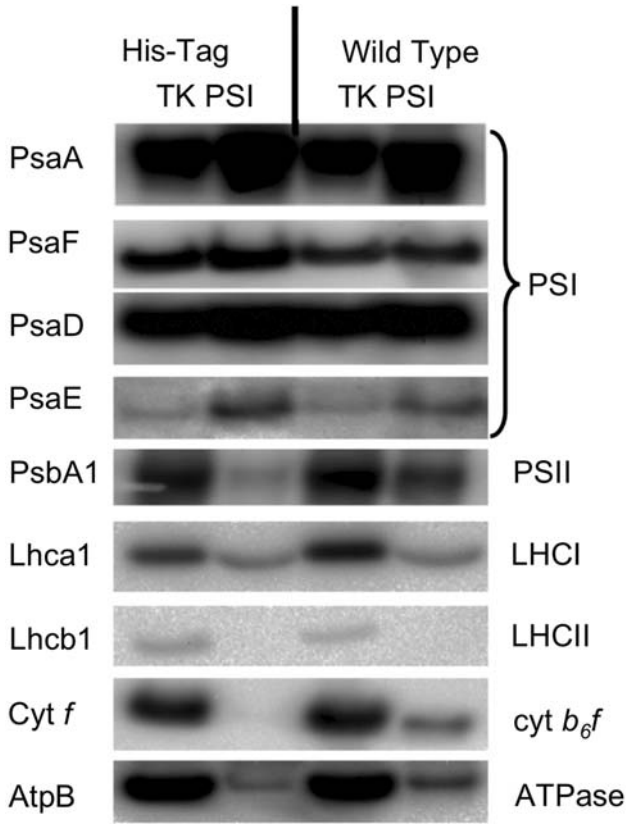

Fig. 5 Immunoblot analysis of H_6-PS1 and conventionally purified WT PS1 particles. Lanes were loaded with equal amounts of Chl (2 μg) from the TK membranes and the PS1 particles isolated from them. Immunoblots were performed with antibodies against the indicated subunits of the major thylakoid membrane protein complexes

isolated, were run on SDS-PAGE gels on an equal Chl basis. The first indication that the affinity-purified H_6-PS1 particles were more pure than PS1 purified by conventional sucrose gradients was the fact that the immunoblot signals from the PS1 subunits were stronger in the lanes from the H_6-PS1 particles (Fig. 5). Contrariwise, as judged by the lower signals from key subunits of the other major thylakoid membrane protein complexes, the H_6-PS1 preparation were less contaminated with PS2 (PsbA), cyt b_6f (cyt *f*), or ATP synthase (AtpB). The content of LHC1, as seen by reaction with the anti-Lhca1 antibody, was very similar to that of conventionally purified PS1, and probably reflects the fact that the LHC1 complexes remain tightly attached to PS1 and are not removed by the relatively gentle conditions used to wash the Ni-NTA column and elute the H_6-PS1 from it.

We measured the amount of photoactive P_{700} in the preparations using flash spectroscopy. Particles were excited with a 30-μs blue flash, and spectroscopic changes in the red region were detected with a second flash of monochromatic light. A transient bleaching that peaked near 699 nm was formed immediately upon the flash, and decayed with a time constant of 110–180 ms in both preparations (data not shown). The spectra of the flash-induced change in the 2 samples were nearly identical (see Supplementary Fig. 1). Based on the published extinction coefficient of 100,000 M^{-1} cm^{-1} for P_{700} in this species (Witt et al. 2003), we could estimate a P_{700} content of 1 per 291–303 Chls in the WT PS1 preparation and 1 per 203–209 Chls in the H_6-PS1 preparation. Thus, the H_6-PS1 preparation was ~40% more pure than the WT PS1 preparation when normalized to total Chl (see Table 1). The pigment composition of the H_6-PS1 preparation compares favorably to that found in highly purified LHCI-PS1 particles from *C. reinhardtii* cells in state 1, which contained 215 Chls, of which 40 were Chl *b* (Kargul et al. 2003). It is thus likely that the H_6-PS1 particles purified from the Ni-NTA column represent PS1 with a tightly attached complement of LHCI. The extra ~90 Chls in the WT PS1 preparation likely originate from loosely attached LHCI or completely unattached pigment proteins. While

Table 1 Properties of PS1 preparations purified by conventional sucrose gradients (WT PS1) or via the His_6-tag (H_6-PS1)

Type of preparation	Chl/P_{700} (mole/mole)	P_{700}/protein (μmol/g)	Chl *a/b* (mole/mole)
H_6-PS1	206 ± 3	1.4 ± 0.02	7.5 ± 0.1
WT PS1	296 ± 7	1.4 ± 0.05	6.7 ± 0.1

both of these are probably true to some extent, the fact that the Chl *a/b* ratio was not much lower in the WT PS1 preparation would indicate that not very much LHC II (with a lower *a/b* ratio) was contaminating the sample (Table 1).

It was important to know if the PS1 preparation contained uncoupled pigments, as these could interfere in spectroscopic studies. Fluorescence emission spectra from the PS1 preparations were taken at 77 K, using excitation at 430 nm (Chl *a*; Fig. 6) or 467 nm (Chl *b*; not shown). LHC purified from the same sucrose gradient used to purify PS1 had a strong emission peak at 678–680 nm. There was only a very minor peak at this wavelength in the His_6-PS1 preparation, which displayed a major peak at 715 nm, with a long tail into the near-infrared (Fig. 6). The conventionally purified PS1 preparation had the same two peaks, but the emission from disconnected LHC-like pigments was much larger. This is likely due to the fact that such preparations can contain unconnected pigment–protein complexes that co-sediment in the gradients. Excitation at 467 nm produced similar emission spectra, except that some pigments fluorescing near the position of free Chl (~650–660 nm; data not shown) were seen in the WT PS1

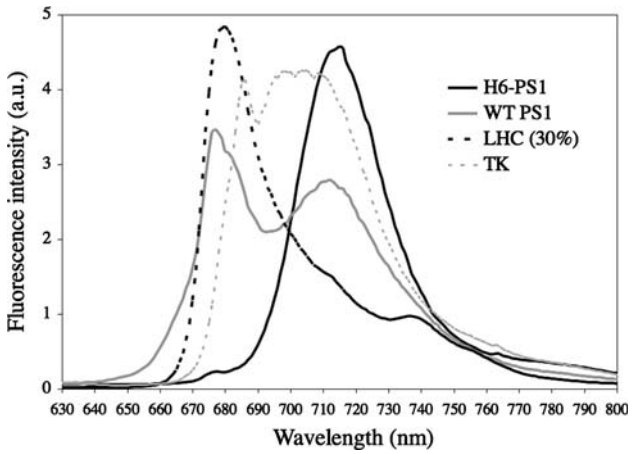

Fig. 6 Low-temperature fluorescence emission spectra of H_6-PS1 particles (solid black line), WT PS1 particles (solid gray line), and LHC (dotted black line), and thylakoid membranes (TK; dotted gray line) using excitation at 430 nm. Samples containing 7.5 μg/ml chlorophyll were frozen in liquid N_2 and measurements were taken at 77 K. (Note that fluorescence from LHC was scaled to 30% to enable comparison)

preparation. This fluorescence analysis indicates that the H_6-PS1 preparation is almost completely lacking in uncoupled pigments, even a small fraction of which can dominate the steady-state fluorescence spectrum due to their long lifetimes (Murakami 1997).

Activity and function of the H_6-PS1

Due to the position of the His_6-tag on the stromal side, we wanted to test the possibility that it could have an effect upon the FeS clusters in PsaC. We used EPR spectroscopy, since it is well-known that the magnetic properties of FeS clusters can be very sensitive to changes in their environment. Purified PS1 particles were frozen in liquid nitrogen while under strong illumination to generate the $P_{700}^{+}F_{A/B}^{-}$ state, which is stable at low temperatures (Lakshmi et al. 1999; Vassiliev et al. 2001). This is a mixed state in which the electron spends most of its time on F_A (Fischer et al. 1997). Neither sample produced EPR spectra before illumination at 9 K, except for a very weak P_{700}^{+} radical signal resulting from the ambient room light (not shown). This was expected, since the oxidized form of the $[4Fe-4S]^{2+}$ clusters should be EPR-silent. When the samples were illuminated in liquid nitrogen, both exhibited signals corresponding to several resonances of the Fe–S clusters and an unresolved asymmetric signal at $g = 2.004$, which is characteristic of P_{700}^{+} in PS1 (Fig. 7). The shape of the EPR signals of the two samples were similar; the better resolution of the signals in the H_6-PS1 sample is likely due to their higher purity, since equal amounts of Chl were present in each tube. Both samples therefore contain photoreduced $[4Fe-4S]^{+}$ clusters (Scott and Biggins 1997). The EPR spectra exhibited no other resonances in the low-field region ($g > 3$), indicating the absence of any high-spin iron (data not shown). Thus, the EPR-active species can be characterized as low-spin ($S = 1/2$) FeS centers with unaltered cysteine ligands (Scott and Biggins 1997). In the H_6-PS1 sample, the EPR resonances observed at $g = 1.84$, ~1.93, and ~2.04 are characteristic of F_A^{-} (Fromme et al. 2002; Jung et al. 1996). Another set of resonances at $g = 1.88$, 1.91 and 2.07 is assigned to F_B^{-}. The *g*-values assigned here to F_A^{-} and F_B^{-} are comparable to those reported for *Synechocystis* sp. PCC6803 under identical conditions (Vassiliev et al. 2001). Although we see the presence of both F_A^{-} and F_B^{-}, the dominance of the F_A^{-} is clearly seen, as expected in this species (Fischer et al. 1997). Therefore we can conclude that there are no major structural changes in the PsaC subunit due to the presence of the His_6-tag.

We measured the photochemical activity of the isolated PS1 particles by O_2 uptake using ascorbate as electron donor and dichlorophenolindophenol as a mediator to PS1,

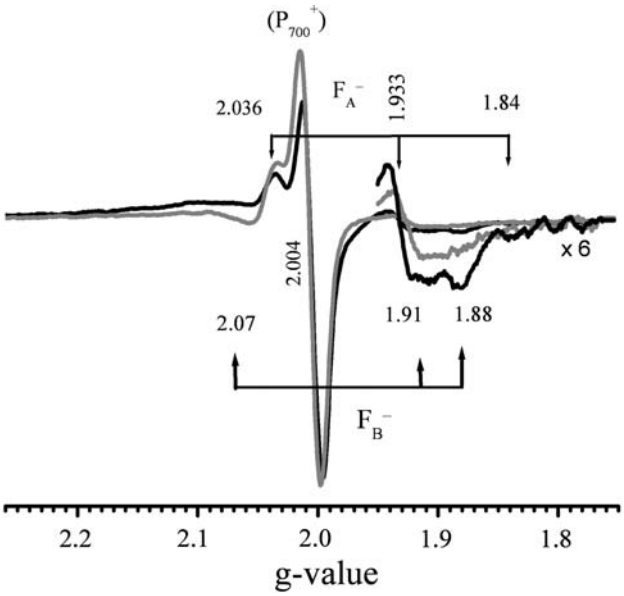

Fig. 7 EPR spectra of the P_{700}^{+} $F_{A/B}^{-}$ state in H_6-PS1 and WT PS1 particles. Particles were frozen under illumination and the EPR spectra of H_6-PS1 (black) and WT PS1 (gray) were measured at 9 K in pulsed mode (see Materials and Methods for details). The derivatives of the absorption spectra were taken to identify the peak positions more clearly. The high-field portion of the spectrum is enlarged 6-fold to enable viewing of g_{yy} and g_{zz} components of the FeS^{-} signals

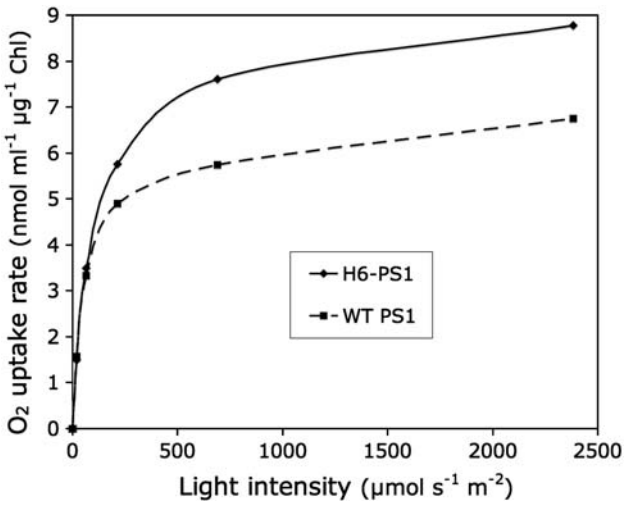

Fig. 8 Photochemical activity of H_6-PS1 (diamonds, solid line) and WT PS1 (squares, dashed line) particles. O_2 uptake was measured at a range of light intensities using a Clark-type electrode and a red LED as actinic light source. Rates are normalized to Chl content

and methyl viologen as a mediator to oxygen. Rates of O_2 consumption were measured at different light fluxes (0–2,400 µEinstein m^{-2} s^{-1}), and the maximal O_2 uptake rate was calculated from double-reciprocal plots. The H_6-PS1 particles possessed a saturated O_2 uptake activity of 8 µmol min^{-1} (µg Chl)$^{-1}$, while that of the WT PS1 particles was 6.1 µmol min^{-1} (µg Chl)$^{-1}$ (Fig. 8). Thus, the H_6-PS1 particles purified by Ni-NTA chromatography are fully active. Their higher specific activity merely reflects their higher purity (on a per Chl basis), in line with our previous observations.

Discussion

In summary, this approach allows a rapid, high-yield purification of PS1. By all measures, the addition of the His_6-tag did not interfere with PS1 function. This was expected, given the location. However, it was gratifying to know that not even by EPR could we detect a significant change in the *g*-tensor of F_A or F_B, given the extreme sensitivity of FeS clusters to changes in their environment (Vassiliev et al. 2001). Thus, this method should be generally applicable to mutants in *C. reinhardtii* and to purification of PS1 from other species. Moreover, the excellent purity afforded by this technique makes it very attractive for a variety of ultra-fast spectroscopic techniques, which can be very sensitive to small amounts of uncoupled pigments, due to their long excited-state lifetimes (Müller et al. 2003). We chose to use dialysis after the purification to remove the imidazole, in order to compare the particles directly to those made by sucrose gradients, which made the total procedure more time-consuming, but the protocol could be made faster using a desalting column and/or simply collecting particles by ultracentrifugation.

Others have experienced good success with the epitope tagging approach for purifying photosynthetic reaction centers (RCs). Attachment of a poly-histidine tag to the bacterial RC allowed recovery of pure protein in <4 h with a Ni-NTA resin (Goldsmith and Boxer 1996). The Ni-NTA resin has also been used to isolate a His_6-tagged PS2 complex from *C. reinhardtii* (Sugiura et al. 1998). There had been at least one previous attempt to tag PS1. Tang and Chitnis (Tang and Chitnis 2000) attached hexahistidyl tags to the C-termini of both PsaK or PsaL in *Synechocystis* sp. PCC6803. However, the tagged PS1 complexes could not be purified on a Ni affinity column without urea pretreatment, indicating that the tags were embedded within the complex. This idea was supported by the fact that the tags were also resistant to trypsin cleavage. This underscores the importance of placing the tag in an accessible place.

Although we likely could have placed the His_6-tag at the N-terminus of PsaB, there was an additional reason to put it at the N-terminus of PsaA. The His_6-tag is now in the first exon of *psaA*. The vast majority of site-directed mutations made in *C. reinhardtii psaA* have been made in the third exon, which encodes the last 661 residues (out of 751). Due to this, we do not need to insert the tag at the DNA level into the pre-existing mutant constructs. Instead, all we need

do is transform the site-directed mutants into the tagged strain (which is no longer antibiotic-resistant), and the *trans*-splicing system will then add the tag automatically as it stitches together exon1 (tagged), exon 2, and exon 3.

Acknowledgments The authors wish to thank Erica Livingston and Lynn Thronson for their contributions to the early stages of the cloning, and Fabrice Rappaport for assistance with the P_{700} photobleaching measurements. This work was supported by an NSF CAREER award (MCB-0347935) to Kevin E. Redding.

References

Amunts A, Drory O, Nelson N (2007) The structure of a plant photosystem I supercomplex at 3.4 Å resolution. Nature 447:58–63

Ben-Shem A, Frolow F, Nelson N (2003) Crystal structure of plant photosystem I. Nature 426:630–635

Boudreaux B, MacMillan F, Teutloff C et al (2001) Mutations in both sides of the photosystem I reaction center identify the phylloquinone observed by electron paramagnetic resonance spectroscopy. J Biol Chem 276:37299–37306

Fischer N, Stampacchia O, Redding K et al (1996) Selectable marker recycling in the chloroplast. Mol Gen Genet 251:373–380

Fischer N, Setif P, Rochaix JD (1997) Targeted mutations in the psaC gene of *Chlamydomonas reinhardtii*: preferential reduction of FB at low temperature is not accompanied by altered electron flow from photosystem I to ferredoxin. Biochem 36:93–102

Fromme P, Bottin H, Krauss N et al (2002) Crystallization and electron paramagnetic resonance characterization of the complex of photosystem I with its natural electron acceptor ferredoxin. Biophys J 83:1760–1773

Golbeck JH, Bryant DA (1991) Photosystem I. In: Lee CP (ed) Current topics in bioenergetics: light driven reactions in bioenergetics. Academic Press, New York

Goldschmidt-Clermont M (1991) Transgenic expression of aminoglycoside adenine transferase in the chloroplast: a selectable marker for site-directed transformation of *Chlamydomonas*. Nucl Acids Res 19:4083–4089

Goldschmidt-Clermont M, Girard-Bascou J, Choquet Y et al (1990) Trans-splicing mutants of *Chlamydomonas reinhardtii*. Mol Gen Genet 223:417–425

Goldsmith J, Boxer S (1996) Rapid isolation of bacterial photosynthetic reaction centers with an engineered poly-histidine tag. Biochim Biophys Acta 1276:171–175

Goldsmith JO, King B, Boxer SG (1996) Mg coordination by amino acid side chains is not required for assembly and function of the special pair in bacterial photosynthetic reaction centers. Biochem 35:2421–2428

Harris EH (1989) The Chlamydomonas sourcebook. A comprehensive guide to biology and laboratory use. Academic Press, San Diego

Henderson JN, Zhang J, Evans BW et al (2003) Disassembly and degradation of photosystem I in an in vitro system are multievent, metal-dependent processes. J Biol Chem 278:39978–39986

Hippler M, Drepper F, Farah J et al (1997) Fast electron transfer from cytochrome c_6 and plastocyanin to photosystem I of *Chlamydomonas reinhardtii* requires PsaF. Biochem 36:6343–6349

Joliot P, Béal D, Frilley B (1980) Une nouvelle méthode spectrophotométrique destinée à l'étude des réactions photosynthétiques. Journal de chimie physique 77:209–216

Jordan P, Fromme P, Witt HT et al (2001) Three-dimensional structure of cyanobacterial photosystem I at 2.5 A resolution. Nature 411:909–917

Jung YS, Vassiliev IR, Qiao F et al (1996) Modified ligands to F_A and F_B in photosystem I. Proposed chemical rescue of a [4Fe–4S] cluster with an external thiolate in alanine, glycine, and serine mutants of PsaC. J Biol Chem 271:31135–31144

Kargul J, Nield J, Barber J (2003) Three-dimensional reconstruction of a light-harvesting complex I-photosystem I (LHCI-PSI) supercomplex from the green alga *Chlamydomonas reinhardtii*. Insights into light harvesting for PSI. J Biol Chem 278:16135–16141

Krabben L, Schlodder E, Jordan R et al (2000) Influence of the axial ligands on the spectral properties of P700 of photosystem I: a study of site-directed mutants. Biochem 39:13012–13025

Kück U, Choquet Y, Schneider M et al (1987) Structural and transcriptional analysis of two homologous genes for the P700 chlorophyll *a*-apoproteins in *Chlamydomonas reinhardtii*: evidence for in vivo *trans*-splicing. EMBO J 6:2185–2192

Lakshmi KV, Jung YS, Golbeck JH et al (1999) Location of the iron-sulfur clusters F_A and F_B in photosystem I: an electron paramagnetic resonance study of spin relaxation enhancement of P_{700}^+. Biochem 38:13210–13215

Müller MG, Niklas J, Lubitz W et al (2003) Ultrafast transient absoprtion studies on photosystem I reaction centers from *Chlamydomonas reinhardtii* I. A new interpretation of the energy trapping and early electron transfer steps in photosystem I. Biophys J 85:3899–3922

Murakami A (1997) Quantitative analysis of 77K fluorescence emission spectra in *Synechocystis* sp. PCC 6714 and *Chlamydomonas reinhardtii* with variable PS I/PS II stoichiometries. Photosyn Res 53:141–148

Perron K, Goldschmidt-Clermont M, Rochaix JD (2004) A multiprotein complex involved in chloroplast group II intron splicing. RNA 10:704–711

Porra R, Thompson W, Kriedemann P (1989) Determination of accurate extinction coefficients and simultaneous equations for assaying chlorophylls *a* and *b* with four different solvents: verification of the concentration of chlorophyll standards by atomic absorption spectroscopy. Biochim Biophys Acta 975:384–394

Ramesh VM, Webber AN (2004) Rapid isolation and purification of photosystem I chlorophyll-binding protein from *Chlamydomonas reinhardtii*. Methods Mol Biol 274:19–28

Redding K, MacMillan F, Leibl W et al (1998) A systematic survey of conserved histidines in the core subunits of Photosystem I by site-directed mutagenesis reveals the likely axial ligands of P700. EMBO J 17:50–60

Redding K, Cournac L, Vassiliev IR et al (1999) Photosystem I is indispensable for photoautotrophic growth, CO2 fixation, and H2 photoproduction in *Chlamydomonas reinhardtii*. J Biol Chem 274:10466–10473

Rochaix JD (1978) Restriction endonuclease map of the chloroplast DNA of *Chlamydomonas reinhardtii*. J Mol Biol 126:597–617

Scott MP, Biggins J (1997) Introduction of a [4Fe–4S (S-cys)4]$^{+1,+2}$ iron-sulfur center into a four-alpha helix protein using design parameters from the domain of the F_x cluster in the Photosystem I reaction center. Protein Sci 6:340–346

Smith P, Krohn R, Hermanson G, Mallia A, Gartner F, Provenzano M, Fujimoto E, Goeke N, Olson B, Klenk D (1985) Measurement of protein using bicinchoninic acid. Anal Biochem 150:76–85

Sugiura M, Inoue Y, Minagawa J (1998) Rapid and discrete isolation of oxygen-evolving His-tagged photosystem II core complex from *Chlamydomonas reinhardtii* by Ni^{2+} affinity column chromatography. FEBS Lett 426:140–144

Takahashi Y, Goldschmidt-Clermont M, Soen S et al (1991) Directed chloroplast transformation in *Chlamydomonas reinhardtii*: insertional inactivation of the psaC gene encoding the iron sulfur protein destabilizes photosystem I. Embo J 10:2033–2040

Tang H, Chitnis PR (2000) Addition of C-terminal histidyl tags to PsaL and PsaK1 proteins of cyanobacterial photosystem I. Indian J Biochem Biophys 37:433–440

Vassiliev IR, Antonkine ML, Golbeck JH (2001) Iron-sulfur clusters in type I reaction centers. Biochim Biophys Acta-Bioenerg 1507:139–160

Witt H, Bordignon E, Carbonera D et al (2003) Species-specific differences of the spectroscopic properties of P700: analysis of the influence of non-conserved amino acid residues by site-directed mutagenesis of photosystem I from *Chlamydomonas reinhardtii*. J Biol Chem 278:46760–46771